Plasma Nonuniformity and Grid Erosion in an Electron Bombardment Ion Engine

DANIEL J. KERRISK* AND T. D. MASEK†
Jet Propulsion Laboratory, Pasadena, Calif.

The plasma in an electron bombardment ion engine of the Kaufman type has been found to be very nonuniform at the ion emission surface. This could lead to a nonuniform sputtering erosion and the destruction of the accelerator grid, because of both poor focusing of the ion beam at some points and nonuniform charge-exchange rates at different radial positions. In the first case, which can be compensated by a variable perveance geometry, the erosion rate would be expected to depend on the ion density N^+ whereas in the latter case it should depend on the product N_0N^+ where N_0 is the neutral particle density. In the present experiments, the plasma density has been measured with a Langmuir probe and the ion beam profile with a Faraday probe. Together with flow-rate measurements, this gives an experimental determination of N_0N^+. Sputtering, as a function of radial position, was measured using a segmented accelerator grid, and variations in the erosion rate were correlated to the variations in N_0N^+. Results indicate that the engine lifetime estimates based on average grid erosion rates will be high by a factor of 2 to 3, considering only the charge-exchange erosion contribution.

I. Introduction

THE electron bombardment ion engine is being studied presently by several groups as a possible source of primary propulsion for spacecraft. Because of its simplicity, its relatively low power consumption, and its adaptability to a wide range of propellants, it offers an attractive prospect for early development and mission use. However, there are several problem areas outstanding in engines of this type, principally affecting their lifetime capabilities. Since mission requirements will demand life expectancies of 10,000 to 20,000 hr, it is important to know precisely what problems are inherent in engines of this type and how the engine performance will be restricted by longevity considerations.

Two major components of the electron bombardment engine have life-expectancy problems. These are the cathode and the accelerator grid. Extensive cathode development work is being conducted at various laboratories, and, at least in the case of cesium as the propellant, it does not seem overly optimistic to predict that 10,000 hr or better cathodes will be available. The problems of cathode development are relatively well defined, and there does not seem to be any fundamental reason why such lifetimes should not be available.

The lifetime of the accelerator grid poses a quite different problem. Here, sputtering erosion caused by high-energy ion impact can cause grid failure well within the needed engine lifetime. Such impingement can come from two sources: direct interception of a portion of the accelerated ion beam and the impingement of high-energy ions created in the ion beam by the charge-exchange process. The first can be eliminated by good optical design of the electrode system, and at least two groups have studied this problem. The question of charge-exchange sputtering, however, has received only the most cursory examination in terms of the peculiar problems of the electron bombardment engine. Specifically, the nonuniformity of the spatial ion distribution in the plasma source can lead to selective erosion of parts of the grid, rendering questionable those approximations utilizing average current densities, neutral effluxes, and impingement rates. This paper deals with the problem of selective erosion and represents an extension of the work reported earlier on the nonuniformity of the plasma density.

Presented as Preprint 64-688 at the AIAA Fourth Electric Propulsion Conference, Philadelphia, Pa., August 31–September 2, 1964; revision received March 22, 1965. This paper presents the results of one phase of research carried out at the Jet Propulsion Laboratory, California Institute of Technology, under Contract No. NAS 7-100, sponsored by NASA. The authors wish, in particular, to express their gratitude to Roy W. Adams for his invaluable assistance in setting up the experiments and collecting the data and for his continuous efforts in furthering this program in every aspect.

* Research Group Supervisor, Advanced Concepts Section. Member AIAA.

† Research Engineer, Advanced Concepts Section.

II. Statement of the Problem

Previous experimental studies with a Kaufman-type electron bombardment ion engine showed the spatial ion distribution in the plasma to be definitely nonuniform.[1] Specifically, the center of the plasma was found to be highly ionized, with the degree of ionization decreasing rapidly as the radial distance increased. This results in two effects, both of which affect grid lifetime. First, since the shape of the plasma boundary depends on both the accelerating voltage and the ion density in the plasma, it is possible that one part of the boundary will produce a defocused ion beam when other parts of the boundary are producing focused beams, thus leading to direct beam interception. This problem has been investigated by the use of variable perveance geometry at both Hughes and EOS.[2,3] The present study indicates that variable perveance is unnecessary and may possibly be detrimental, as will be shown later.

The second effect is not so amenable to correction and may prove the more serious in limiting engine lifetime. If the total plasma density is uniform across the boundary, a decrease in ion density must be complemented by an increased neutral particle density. These neutrals, effluxing from the engine, form the targets for the charge-exchange process. Assuming that the spatial distribution of neutrals in the accelerating region can be expected to follow that in the engine, the impingement currents can also be expected to vary across the accelerator grid.

The criteria for grid failure can be said to be either when the grid has been totally worn through at any place or when the apertures have become sufficiently enlarged to cause defocusing and direct interception at any place. Thus, if any one area is selectively eroded, an over-all grid average erosion rate would give an erroneous estimate of grid life expectancy.

The purpose of the investigation reported here was to examine the problem of selective erosion. To accomplish this, a standard Kaufman-type engine was employed with a con-

stant perveance grid system. Measurements of plasma composition were made and correlated to beam current distribution, and sputtering rates were measured at various locations on the grid. The details of the experiments performed and the results obtained are presented in the following sections.

III. Approach to the Problem

To determine the extent to which selective erosion will be a problem, and to evaluate its relation to plasma nonuniformity, several bits of information are required. These include the ion density distribution in the plasma, the beam current density profile that must be correlated with the ion density, and the actual erosion losses as a function of radius.

To obtain the ion density distribution in the plasma, a movable Langmuir probe was installed in the engine. From the Langmuir probe characteristic, the salient features of the plasma, such as electron temperature, electron energy distribution, and electron and ion densities could be determined.

The beam profile was measured with a Faraday probe that could be accurately positioned in the beam at locations corresponding to the positions of the Langmuir probe. By comparing the data obtained from these two measurements, beam current density could be correlated to the ion density in the plasma.

Neutral particle density in the accelerating region was computed by using the measured mass flow rate and beam current and by assuming that the neutral distribution in the plasma complemented that of the ions and had a purely thermal exit velocity. Total particle density was assumed uniform across the grid and computed from the known flow rate and beam current.

Using the measured values of beam current density and the computed neutral efflux distribution, the expected charge-exchange current per aperture was computed. The charge-exchange cross section was obtained from Ref. 4.

Finally, using these computed charge-exchange currents and trajectory data taken from Ref. 3, the expected impingement currents were computed as a function of the radius. From this and the sputtering coefficients, the expected erosion rates could be calculated. These were then compared to erosion rates actually measured on a segmented accelerator grid.

IV. Experimental Setup

A Kaufman-type electron bombardment ion engine, purchased from the Ion Physics Corporation, was used in this investigation. This is the same engine described in Ref. 1, and utilizes mercury as the propellant. Two probes, a Langmuir probe for investigating the plasma inside the source and a Faraday probe for determining beam profile, were employed. Both probes could be moved during operation. A schematic of the engine, probes, and associated electrical equipment is shown in Fig. 1. The entire experiment was mounted in a 3×7-ft vacuum chamber capable of attaining pressures of 1×10^{-7} torr. During operation, pressure was normally about 3×10^{-6} torr.

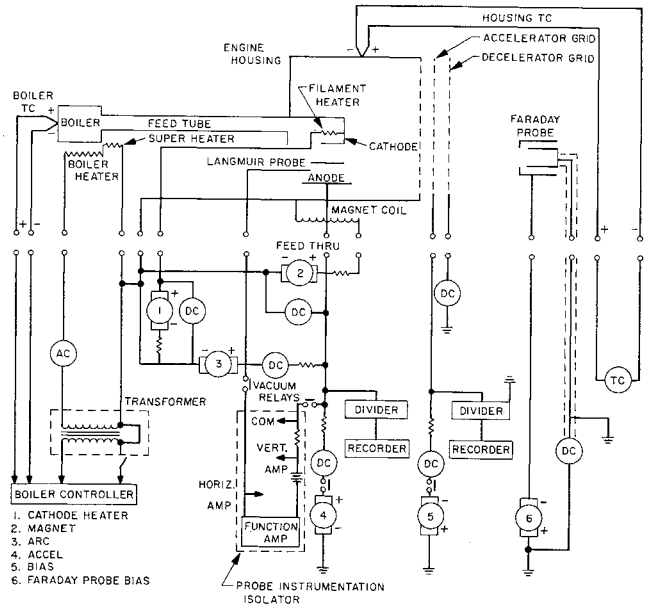

Fig. 1 Circuit diagram of engine and probes.

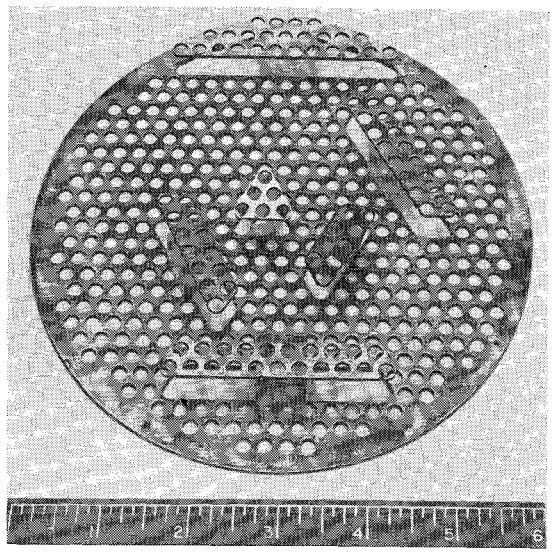

Fig. 2 Segmented copper accelerator grid.

For the sputtering experiment, a segmented copper accelerator grid was used. Copper was chosen because of its high sputtering coefficient.[5,6] This grid is shown in Fig. 2. Carefully fitted removable segments were positioned as shown at various radial distances, permitting weight loss of the grid to be measured as a function of the radius.

The Langmuir probes used in this work were made from 0.020-in. tungsten wire and quartz tubing. A typical probe is shown in Fig. 3. The Langmuir probes are adjustable to 25 positions in the engine as illustrated in the figure. The Faraday probe used in the ion beam is shown mounted with the engine in Fig. 4. This probe has a 0.060-in. entrance aperture and can be adjusted to 13 positions 0.5 in. apart radially and 13 axial positions 0.5 in. apart. The outer case of the Faraday probe is biased negatively to suppress secondary electrons. The collecting element is molybdenum within a boron nitride cylinder used to insulate the collector from the outer case.

The mechanisms for positioning the probes are shown on the vacuum tank header in Fig. 5. These mechanisms allowed the probes to be located with good accuracy and repeatability.

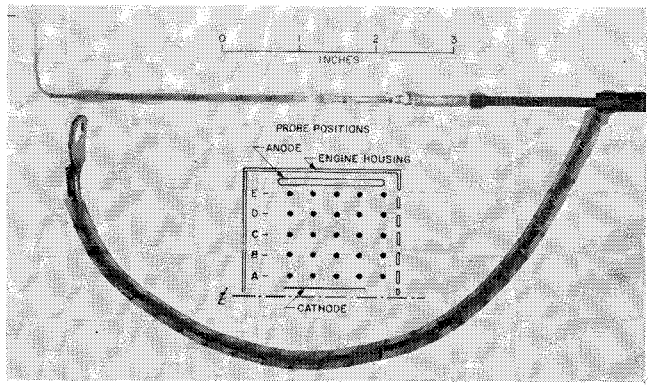

Fig. 3 Movable Langmuir probe; insert shows probe positions in engine.

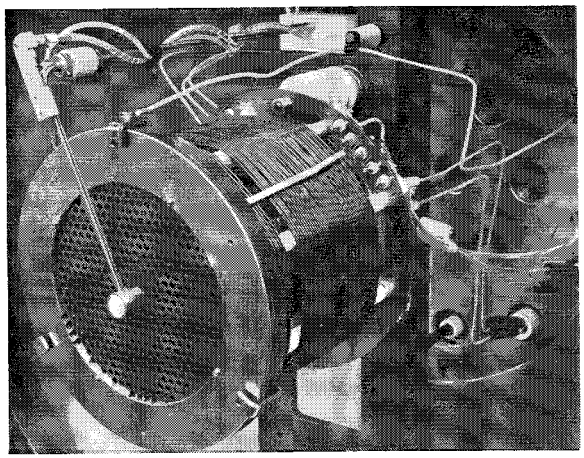

Fig. 4 Movable Faraday probe mounted with engine.

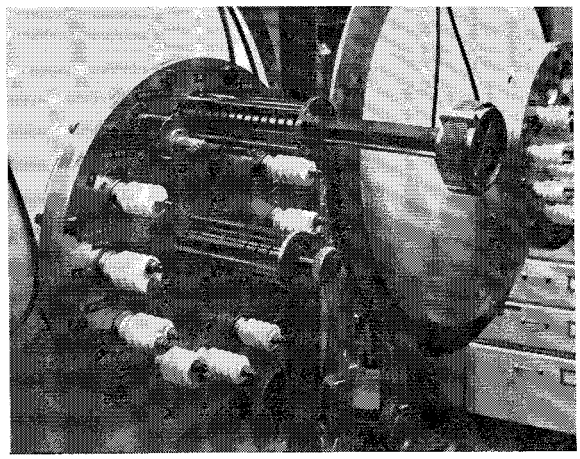

Fig. 5 Probe adjustment mechanisms; lower positioner is for Langmuir probe, and upper positioner is for Faraday probe.

The instrumentation for the Langmuir probe consisted of a 0- to 250-v d.c. power supply, variable frequency function generator, cathode follower amplifier, x-y plotter, bias batteries, and a 5-ohm shunt. This instrumentation was at high voltage during engine operation and was coupled to the engine through vacuum relays. This allowed the instrumentation to be decoupled without disturbing the engine operation.

The Faraday probe operated at ground potential, so that instrumentation was simplified, and consisted of a microammeter and 0- to 250-v d.c. power supply.

V. Experimental Procedure

A. Mass Flow Rate Determination

Mass flow rate was determined by weight measurements before and after each run. An analytical balance accurate to 0.1 mg was used to determine the weight lost during the run. While in operation, the boiler temperature was controlled by means of a saturable core reactor to approximately $\pm 2°$F, and this temperature was monitored constantly on a strip chart recorder.

Since the various runs were interrupted at times by shutdowns, a correction was made for start-up and shutdown times. Typically, the boiler required about 15 min to come up to operating temperature and would decay to less than 5% of operating flow rate in about 20 min. No valves were employed.

Whereas run lengths varied from 16 to 70 hr, continuous periods of operation ranged only from 2 to 12 hr. Based on the accuracy of the weight measurements and the percentage of the total time involved in the start-up and shutdown periods, the flow-rate measurements are considered to be accurate to no worse than $\pm 2\%$.

B. Procedure During Operation

The start-up procedure involved first bringing the cathode up to emitting temperature. The boiler controller would then be activated, and while the boiler warmed up the high voltage was applied. As soon as possible during the warm-up period the arc would be struck, typically when the boiler temperature was about 525°F. The beam then came up as the boiler approached its set point. In general, the arc voltage and the cathode temperature were set to predetermined values. The magnet current was then adjusted to give the maximum beam current. Thereafter, the beam current was regulated by adjusting the cathode temperature.

During the course of a run, the various readout meters were monitored approximately every half hour, and the cathode adjusted as necessary to bring the operating conditions back to nominal. Beam current variations as high as $\pm 5\%$ (or about ± 10 ma) were observed, presumably because of changes in the cathode emission.

Langmuir and Faraday probe measurements were taken on the average of twice a day to detect variations in the plasma characteristics and the beam. The probe curves were taken at maximum and minimum beam values, as well as at the set point to see the effect on the plasma of the cathode variations.

C. Sputtering Rate Determination

Sputtering rates were determined by measuring mass loss during a run. Segments were cleaned and weighed carefully on an analytical balance just prior to installation of the engine into the vacuum tank. During the run, interception currents on the accelerator grid were monitored, and in almost all cases were less than 0.5% at the start of the run, although during the longer runs this would increase to almost 1%. After the run, the segments were again removed from the grid for weighing. Invariably there would be back-sputtered material, either from the ion beam collector or from the decelerator grid when it was employed. The ion collector sputtered back titanium, which was found to be easily removable; generally it flaked off. The decelerator grid was of graphite, and the sputtered graphite was removed by cleaning it in a solution of acetone and concentrated hydrochloric acid. The segments were then weighed and examined microscopically. The latter was felt to be necessary if we were to have confidence that the weight losses measured did indeed come from charge-exchange sputtering rather than either direct interception or loss in the cleaning process. To verify the latter, unsputtered copper was subjected to the same cleaning process and examined. No detectable change was observed in the microscopic structure of the copper surface.

VI. Experimental Results

A total of four runs was made during the course of this investigation at varying conditions of flow rate, beam current, and beam extraction. Run 1 was of short duration, and the results were inconclusive. The remaining three runs provided the data presented here. The salient parameters for each run are given in Table 1. These are the nominal values; it should be noted that I_{arc} and I_{beam} varied by about 5% around these values.

To correlate plasma nonuniformity with sputtering rates, it is necessary to know the ion and neutral particle density

Table 1 Operating parameters for the electron bombardment engine during sputtering experiments

Run	$\dot{m}$, g/hr	V_{arc}, v	I_{arc}, amp	I_{mac}, amp	V_{accel}, kv	V_{bias}, kv	I_{beam}, ma	η_p, %
1	1.49	30	4.5	6.7	3.0	1	150	...
2	1.90	35	5.5	6.4	3.0	1	200	79
3	1.90	45	3.0	7.5	3.5	2	215	85
4	1.90	45	3.1	7.5	3.5	2	230	91

distributions in the plasma and the current density distribution in the beam as well as the sputtering distribution across the grid. The Langmuir and the Faraday probes were used to obtain the ion density and beam current density distributions, respectively. The assumption of constant total density was then used to obtain the neutral density distribution.

For the purpose of interpreting the data, the grid area was divided into six concentric rings of outer diameters, respectively, 1, 2, 3, 4, 5, and 6 in. In Fig. 6, these rings are shown, with the positions where the Langmuir and Faraday probe measurements were taken. Superimposed on the rings are the six segments used for the sputtering determination. In the succeeding sections and illustrations of this paper, the area and probe position designations are referenced to the positions shown on this figure.

A. Langmuir Probe Results

The Langmuir probe characteristics showed the typical behavior for nonuniform three-component plasma (i.e., plasma in which a high-energy electron group can be distinguished from the Maxwellian group) as reported earlier in Ref. 1. Since the method of analyzing these characteristics is gone into in detail in that paper, it will not be repeated here. The ion density distributions for the various runs, as determined by the referenced method, are shown in Fig. 7.

B. Faraday Probe Results

The Faraday probe was used to obtain beam profiles that could be correlated to the ion density and used to obtain the ion exit velocities and the current density in the accelerator region. In the axial positions nearest the grid, the profile was observed to be very ragged, which was interpreted to mean the ion beams from the various apertures had not yet mixed completely. As the axial distance was increased, the profiles smoothed out considerably, which would tend to verify this assumption. A typical set of such profiles from run 3 is shown in Fig. 8.

Some difficulty with voltage breakdown was experienced when the probe was in the axial position nearest the grids, and most data were taken from position 2 outwards. From the decay of the peak, it was possible to extrapolate back to the grid station, as shown in Fig. 9. These curves were then divided by the entrance aperture to the probe to determine the beam current density profile. After correction for the void areas between holes, the current density through the apertures was obtained. This current density profile compared very well on integration with the beam current, and, when divided by the plasma ion density, indicated ion exit velocities of the order of 1.5 to 2 ev. These velocities seemed quite reasonable, since the ions in the plasma will have directed velocities at the grid due to residual fields in the plasma.

The ion beam profiles extrapolated to the grids are given for the various runs in Fig. 10. These profiles are for the nominal operating parameters for each run and represent a reasonable average of the various profiles found as the arc parameters

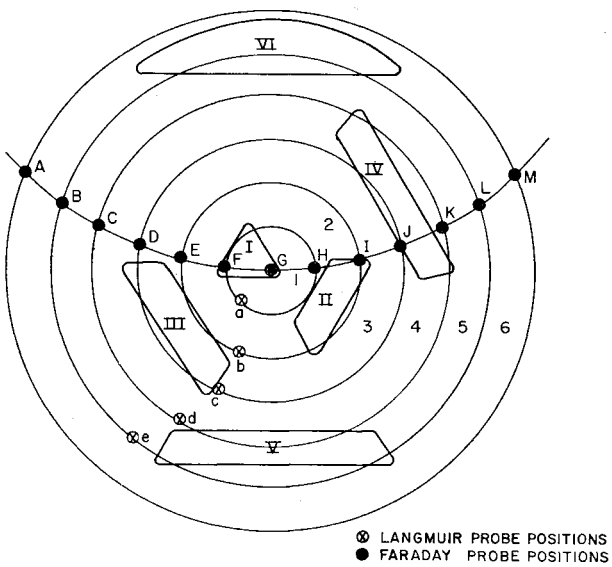

Fig. 6 Segmented accelerator grid layout with Langmuir probe and Faraday probe radial position indicated.

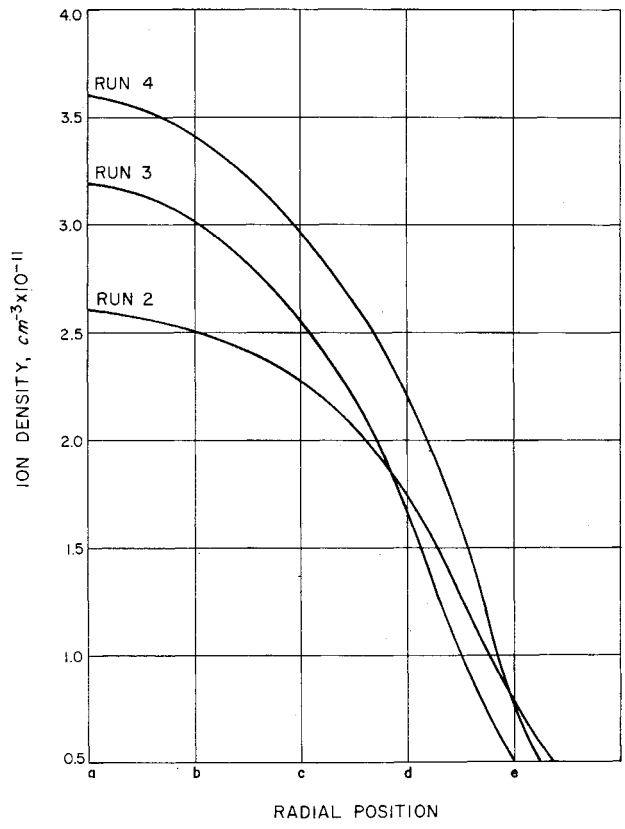

Fig. 7 Ion density distribution in plasma at grid position for three runs.

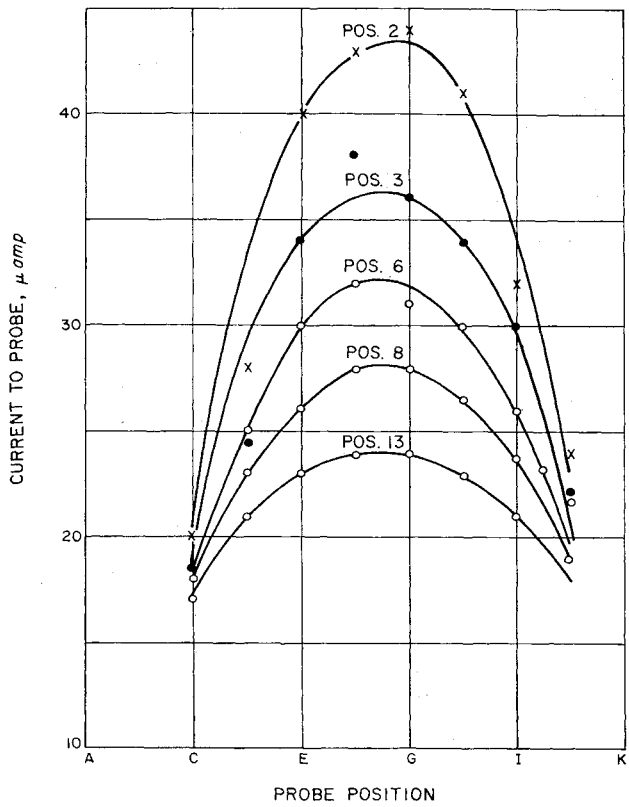

Fig. 8 Faraday probe distribution at various axial positions. Position 2 is 0.5 in. from decelerator grid for run 3.

drifted. These current densities were then used in the calculation of expected sputtering rates from charge exchange.

C. Sputtering Results

Two major concerns in the sputtering study were the elimination of direct interception as a source of sputtering and the obtaining of accurate mass loss measurements when the segments had to be cleaned of back-spattered material after a run. The first could only be done by inference; in preparatory runs, without the segmented bias grid, accelerator and bias voltages were varied to obtain minimum drain currents on the bias grid. These were then used during the actual run.

It was also expected that any direct interception would be concentrated around the apertures, whereas charge-exchange sputtering would be more or less evenly distributed between the apertures. This latter conclusion was based on the trajectory study for charge-exchange particles done at Hughes.[3] No noticeable increase in damage was found at the edge of the apertures, lending credence to the belief that at least the major part of the weight loss was due to charge-exchange sputtering.

The accuracy of the mass loss measurement, however, poses a difficult question. During operation without the decelerator grid, the segmented copper grid was exposed to a titanium back sputtered from the ion beam collector located abou 4 ft away. After runs 1 and 2, the grid was found to be coated with titanium, which had to be removed before weight measurements could be made. It was found that the titanium came off fairly easily, most of it flaking off, but some remained, especially on the sides of the apertures, and it was difficult to estimate how much was left on. In order to protect the segmented grid, in runs 3 and 4 a decelerator grid of graphite was used, and the duration of the runs increased to minimize the error caused by foreign material that could not be removed. After running with the decelerator grid, it was found that direct interception at the outside edge of the decelerator grid had coated the accelerator grid with graphite. This could largely be removed with a solution of acetone and concentrated hydrochloric acid, but again some material was left. Microscopic examination of the surface indicated the layers remaining were on the order of 1 to 2 μ in depth, and careful estimation led to an area coverage of less than 0.5 cm^2. Using the density of graphite, this led to an expected error on the order of a few tenths of a milligram. Since weight losses measured several milligrams, the uncertainty in the measurement due to foreign materials is thought to be around 5%.

Another source of error more difficult to assess is the protective action of a layer of back-sputtered material on the accel electrode. The correspondence between calculated and measured sputtering rates would indicate that this effect was small, but in any event it would not affect the weight loss distribution, only its absolute magnitude.

Figure 11 presents the sputtering rates found in this investigation. The exposure times for each run are noted on the graphs. The results are area normalized; the area used in determining the loss per cm^2 was the total area exposed, including the upstream and downstream faces and the sides of the apertures. Although no microscopic examination could be made of the sides of the apertures, there was no qualitative difference in the appearance of the upstream and downstream

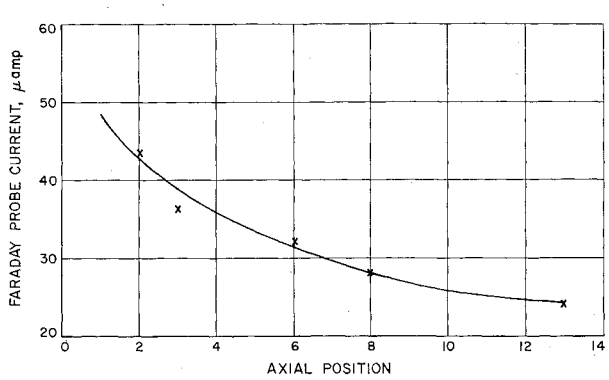

Fig. 9 Decay of Faraday probe maximum current with axial distance.

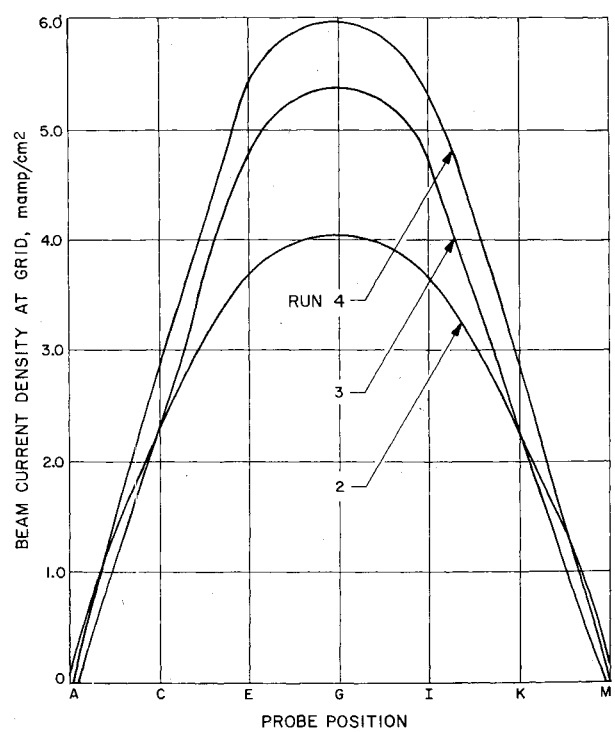

Fig. 10 Faraday probe beam profile at accelerator grid for three runs.

faces. It was not possible to make a quantitative estimate of the mass loss distribution between the faces.

VII. Discussion

In the previous section, the experimental findings were reported. It still must be shown that these findings are consistent; i.e., from the observed plasma ion density and beam distribution, it is possible to predict the observed sputtering characteristics.

The total weight loss by charge-exchange sputtering can be approximated by

$$\Delta W/\Delta t = kI_{CE} = k \int\int J(r,x) N_A(r,x) \sigma_{CE}(x) 2\pi r dr dx \quad (1)$$

where $J(r, x)$ is the beam current density at the position r, x, in amperes/centimeters^2; $N_A(r, x)$ is the neutral particle density in the accelerating region at position r, in centimeters^{-3}; $\sigma_{CE}(x)$ is the charge-exchange cross section at position x, in centimeters^2; r is the radial distance measured from the center of the engine, in centimeters, x is the axial distance measured from the emission surface, in centimeters; and k is the average sputtering ratio for the impacting ions, in grams/ampere hours.

If variations in J and N_A with x are neglected, then ΔW will be directly proportional to the integral of the product $J(r)N_A(r)$.

$$\Delta W/\Delta t = K \int J(r) N_A(r) 2\pi r dr \quad (2)$$

where K is a new proportionality constant. Equation (2) can in turn be approximated by the summation

$$\frac{\Delta W}{\Delta t} = K \sum_i J_i N_{A_i} A_i \quad (2a)$$

or the change in weight for each segment is

$$\Delta W_i/\Delta t = K J_i N_{A_i} A_i \quad (3)$$

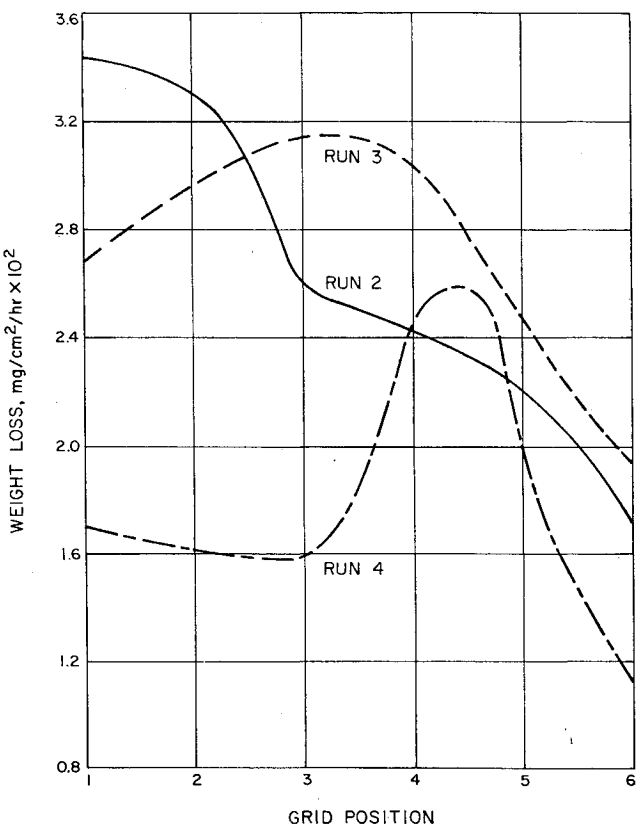

Fig. 11 Experimental sputtering distribution on copper accelerator grid for 3 runs.

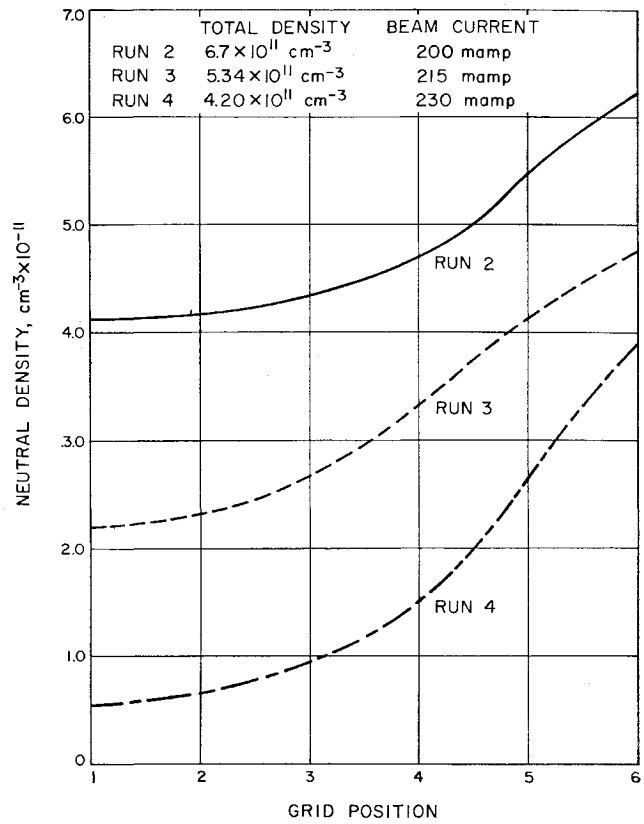

Fig. 12 Neutral particle density distribution in plasma at grid position for 3 runs.

The expected sputtering distribution can then be calculated if the N_{A_i} and J_i are known. The latter are obtained directly from the Faraday probe data. The N_{A_i} can be obtained from the Langmuir probe data, the mass flow rate, and the beam current if certain assumptions are made.

First, if one assumes that the total particle density is constant across the emitter grid, then

$$N_{P_i} = N_T - N_i^+$$

where N_{P_i} is the neutral particle density in the plasma at position i, N_T is the total particle density, and N_i^+ is the ion density at position i. The mass flow rate is given by

$$m = I_B M/e + M N_P = I_B M/e + M \sum_i N_{P_i} A_i \bar{v}/4 \quad (4)$$

where I_B is the beam current, M is the mass of the mercury atom, e is the electronic charge, and $\bar{v}$ is the mean Maxwellian velocity of the neutrals. Using the assumption of constant total density, Eq. (4) can be written as

$$m = I_B M/e + M\bar{v}/4 N_T \sum_i A_i - \sum_i N_i^+ A_i \quad (5)$$

Equation (5) can be solved for N_T, and the N_{P_i}'s can be determined if the value of $\bar{v}$ is known. $\bar{v}$ depends on the temperature of the plasma, which could not be measured directly; a value of 900°K was assumed based on the observed housing temperature of 700°K and expected heat-transfer rates. The calculated values for N_T and N_{P_i} are given in Fig. 12.

Having obtained the plasma neutral density distribution, it was assumed that the neutral distribution in the accelerator region would be proportional to it. Then the total neutral efflux was given by

$$N_0 = \bar{v}_A/4 \sum_i N_{A_i} A_i + N_{A_6} A_7$$

where A_7 is the area for lateral egress from the interaction

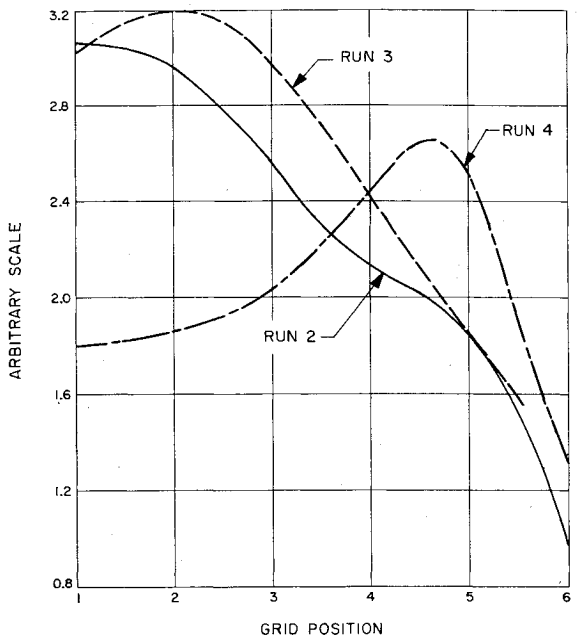

Fig. 13 $N_A J_i$, product of current density and neutral density with arbitrary scale for 3 runs.

region. By dividing through by N_{A_6} and using the assumed proportionality, one obtains

$$N_0 = \frac{\bar{v}_A}{4N_{0_6}}\left[\sum_i N_{P_i}/N_{P_6}A_i + A_7\right] \qquad (6)$$

where $\bar{v}_A$, the mean velocity of neutrals in this region, is obtained from Maxwellian theory for particles emerging through an aperture from a gas, whose mean particle velocity is $\bar{v}$. Specifically, $\bar{v}_A = 3\pi\bar{v}/8$.

From Eq. (5), N_{A_6} was obtained, and the remaining N_{A_i} were obtained from the assumed proportionality to the N_{P_i}. The weight loss distribution for the various cases were then obtained from Eq. (3). These results are plotted in Fig. 13.

A comparison of the experimental curves and the theoretical curves show remarkably good agreement qualitatively. In particular, the increasing radial position of the sputtering peak follows the predicted value based on $J_i N_{A_i}$ quite well. This, however, is still insufficient; it is desirable to have some assurance that the quantitative behavior of the sputtering at least approximates reasonable values for the K of Eq. (3).

The charge-exchange cross section for mercury is not well known; the value used here is taken from Ref. 4 and is assumed to be 0.8×10^{-14} cm^2. This was used as an average value over the interaction region; it can be seen in the reference that the cross section decreases very rapidly with increasing energy.

From run 1, the value of $\Sigma N_{A_i} J_i A_i \sigma_{CE} x$, which should give the total charge-exchange current, is 0.50 ma. This compares favorably with the observed drain current on the bias grid of about 0.85 ma. The difference could be accounted for by secondary electron emission, thermionic electronic emission, and leakage currents. Of these, the thermionic emission may be the greatest contributor; the observed rise in the bias-drain current with time could be due to a gradual heating of the copper electrode. If the curve given in Ref. 3 for normal copper surfaces is to be believed, then for bias electrode temperatures on the order of 350° to 400°C, the expected thermionic emission would account for all differences between the observed and the calculated charge-exchange interception currents. Thermal expansion and the resulting direct impingement are believed to be small because of the lack of typical direct intercept type erosion.

For the assumed charge-exchange average cross section, the average impact energy of the impacting ions would be about 1 kv. For this impact energy, Wehner's results were extrapolated to give a sputtering ratio of about 2 atoms/ion. From the data obtained here and the calculated interception current, a number of 1.25 atoms/ion was found. For the conditions of this experiment the agreement is considered sufficient to support the thesis that indeed charge exchange is being observed and that the observed sputtering distributions can be directly related to the plasma ion density.

VIII. Conclusions

The experiments described here were performed to see if nonuniform sputtering patterns would result from plasma nonuniformities, and if so, to determine how serious they might be. The results indicate that maximum sputtering rates in the cases studied were about 50% higher than the average rates. In addition, if no defocusing was assumed, the lifetime of this particular grid would have been of the order of 12,000 hr before half the grid was eroded away at the position of maximum sputtering. This is based on the results of run 4, which gave the minimum sputtering.

From this, one can conclude that nonuniformity in the sputtering distribution can be expected, and, for the cases studied here, it possibly could be eliminated as a problem by proper design. It should be noted, however, that the maximum current density used here was about 6 ma/cm^2, with an average current density through the apertures of 2.7 ma/cm^2. Pushing to higher current densities at the same utilization efficiency would decrease lifetime in proportion to the square of the current density increase. At an average current density of 10 ma/cm^2, grid life would drop to about 1000 hr.

On the other hand, the photomicrographic examination indicated the damage to be relatively uniform over the surface, and so, the danger of the aperture enlargement and subsequent defocusing is minimized. The lifetime capability at high utilization efficiency is quite high, even for copper, and would be considerably improved by use of molybdenum or other low sputtering materials.

A second conclusion should be noted. If indeed the sputtering damage will follow the product $N_{A_i} J_i A_i$, then there is a danger in variable perveance geometries, which must be considered. For example, in the very efficient run, if $J_i A_i$ is kept constant, then the ratio of sputtering volume to area being sputtered increases rapidly, and the sputtering ratio would vary by almost an order of magnitude. The average sputtering rates would then be much further off than they apparently are in the constant perveance case. Lastly, the assumption of constant total density seems reasonable, considering the good correlation of theory and experiment.

References

[1] Strickfaden, W. B. and Geiler, K. L., "Probe measurements of the discharge in an operating electron bombardment engine," AIAA J. **1**, 1815–1823 (1963).

[2] Speiser, R. C., Worlock, R. M., Barcatta, S. A., Reid, G. C., and Sohl, G., "Ion rocket engine system research and development," Final Report, NASA Contract NAS3-2516 (1964).

[3] Brewer, G. R., "Electrostatic rockets—engine design and performance," Univ. of California at Los Angeles, Course X458 1 (Summer 1963).

[4] Rapp, D. and Francis, W. E., "Charge exchange between gaseous ions and atoms," J. Chem. Phys. **37**, 2631–2645 (1962).

[5] Wehner, G. K., "Low-energy sputtering yields in Hg," Phys. Rev. **112**, 1120–1124 (1958).

[6] Wehner, G. K. and Rosenberg, D., "Mercury ion beam sputtering of metals of energies 4–15 Kev," J. Appl. Phys. **32**, 887–890 (1961).